The Journal of Immunology

Cutting Edge: Caspase-8 Is a Linchpin in Caspase-3 and Gasdermin D Activation to Control Cell Death, Cytokine Release, and Host Defense during Influenza A Virus Infection

Yaqiu Wang, Rajendra Karki, Min Zheng, Balabhaskararao Kancharana, SangJoon Lee, Sannula Kesavardhana, Baranda S. Hansen, Shondra M. Pruett-Miller and Thirumala-Devi Kanneganti

J Immunol 2021; 207:2411-2416; Prepublished online 18 October 2021;
doi: 10.4049/jimmunol.2100757
http://www.jimmunol.org/content/207/10/2411

The Journal of Immunology is published twice each month by
The American Association of Immunologists, Inc.,
1451 Rockville Pike, Suite 650, Rockville, MD 20852

Print ISSN: 0022-1767 Online ISSN: 1550-6606.

Cutting Edge

The Journal of Immunology

Cutting Edge: Caspase-8 Is a Linchpin in Caspase-3 and Gasdermin D Activation to Control Cell Death, Cytokine Release, and Host Defense during Influenza A Virus Infection

Yaqiu Wang,* Rajendra Karki,* Min Zheng,* Balabhaskararao Kancharana,* SangJoon Lee,* Sannula Kesavardhana,*,[1] Baranda S. Hansen,† Shondra M. Pruett-Miller,† and Thirumala-Devi Kanneganti*

Programmed cell death (PCD) is essential for the innate immune response, which serves as the first line of defense against pathogens. Caspases regulate PCD, immune responses, and homeostasis. Caspase-8 specifically plays multifaceted roles in PCD pathways including pyroptosis, apoptosis, and necroptosis. However, because caspase-8–deficient mice are embryonically lethal, little is known about how caspase-8 coordinates different PCD pathways under physiological conditions. Here, we report an anti-inflammatory role of caspase-8 during influenza A virus infection. We generated viable mice carrying an uncleavable version of caspase-8 (*Casp8*$^{DA/DA}$). We demonstrated that caspase-8 autoprocessing was responsible for activating caspase-3, thereby suppressing gasdermin D–mediated pyroptosis and inflammatory cytokine release. We also found that apoptotic and pyroptotic pathways were activated at the same time during influenza A virus infection, which enabled the cell-intrinsic anti-inflammatory function of the caspase-8–caspase-3 axis. Our findings provide new insight into the immunological consequences of caspase-8–coordinated PCD cross-talk under physiological conditions. ***The Journal of Immunology*****, 2021, 207: 2411–2416.**

Innate immunity acts as the first line of defense against invading pathogens. A key component of the innate immune response is programmed cell death (PCD), which can eliminate infected cells and prevent pathogen replication and spread. Because aberrant activation of PCD can cause inflammation and pathology, regulation of PCD pathways is critical for organismal homeostasis. Caspases are key proteins in the regulation of PCD pathways. Caspase-8 in particular is one of the most versatile caspases and is involved in regulating all three of the most well-defined PCD pathways: pyroptosis, apoptosis, and necroptosis. Caspase-8 is essential for both canonical and noncanonical Nod-like receptor family pyrin domain-containing 3 (NLRP3) inflammasome activation (1) and can play a role in gasdermin D (GSDMD)-mediated IL-1β and IL-18 release and pyroptosis (2, 3). It also acts as an initiator caspase downstream of death receptors to activate caspase-3 and -7 for apoptosis (4). Furthermore, it inhibits necroptosis by cleaving receptor interacting serine/threonine kinase (RIPK) 1 (RIPK1) (5). Despite these known roles, study of caspase-8 in vivo has been hindered by a lack of genetic tools. Mice lacking caspase-8 undergo embryonic lethality that can be rescued by additional deletion of *Ripk3* (6, 7); therefore, study of caspase-8 has been limited to studies with *Casp8*$^{-/-}$*Ripk3*$^{-/-}$ mice, which prevents identification of the role of caspase-8 under circumstances where RIPK3 is also functionally involved. Due to the critical roles of RIPK3 in both necroptotic and many nonnecroptotic contexts (8), the function of caspase-8 and the PCD pathways regulated by it under such physiological conditions has not been well-defined.

Influenza A virus (IAV) infection is a global health threat that continues to cause significant outbreaks every year. PCD pathways play an important role in the host response to IAV, and this virus has been shown to trigger pyroptosis, apoptosis, and necroptosis (PANoptosis), which is controlled by the master regulator Z-DNA-binding protein 1 (ZBP1) (9). Downstream

*Department of Immunology, St. Jude Children's Research Hospital, Memphis, TN; and †Center for Advanced Genome Engineering, St. Jude Children's Research Hospital, Memphis, TN

[1]Current address: Department of Biochemistry, Indian Institute of Science, Bengaluru, Karnataka, India.

ORCIDs: 0000-0002-6827-5495 (Y.W.); 0000-0003-4436-9128 (R.K.); 0000-0002-0343-3368 (M.Z.); 0000-0002-1362-4942 (B.K.); 0000-0002-3793-585X (S.M.P.-M.); 0000-0002-6395-6443 (T.-D.K.).

Received for publication August 4, 2021. Accepted for publication September 15, 2021.

This work was supported by grants from the National Institutes of Health (AI101935, AI124346, AI160179, AR056296, and CA253095) and by the American Lebanese Syrian Associated Charities (to T.-D.K.).

Address correspondence and reprint requests to Thirumala-Devi Kanneganti, Department of Immunology, St. Jude Children's Research Hospital, MS #351, 262 Danny Thomas Place, Memphis, TN 38105-2794. E-mail address: Thirumala-Devi.Kanneganti@StJude.org

The online version of this article contains supplemental material.

Abbreviations used in this article: ASC, apoptosis-associated speck-like protein containing a caspase recruitment domain; BMDM, bone marrow-derived macrophage; CST, Cell Signaling Technology; GSDMD, gasdermin D; GSDME, gasdermin E; hpi, hour postinfection; IAV, influenza A virus; MOI, multiplicity of infection; NLRP3, Nod-like receptor family pyrin domain-containing 3; PCD, programmed cell death; RIPK, receptor interacting serine/threonine kinase; WT, wild-type; ZBP1, Z-DNA-binding protein 1.

www.jimmunol.org/cgi/doi/10.4049/jimmunol.2100757

of ZBP1 sensing of IAV, the ZBP1-PANoptosome is formed, which contains key components from pyroptosis (the NLRP3 inflammasome), apoptosis, and necroptosis (10). Formation of the inflammasome triggers caspase-1 activation, release of IL-1β and IL-18, and cell death (11). Inflammasome activation is vitally important to protect the host during IAV infection, as mice deficient in *Nlrp3*, *Pycard* (gene encoding the inflammasome adaptor protein apoptosis-associated speck-like protein containing a caspase recruitment domain [ASC]) or *Casp1* are all highly susceptible to IAV infection (12, 13). Additionally, mice deficient in *Il1r1* and *Il18* also exhibit defects in controlling viral titer (13–15), suggesting that inflammasome-mediated cytokine maturation and release from pyroptotic cells is critical in host protection. Given the central role of caspase-8 in regulating PCD pathways and NLRP3 inflammasome activation and the importance of inflammasome activation in host defense during IAV infection (1, 9, 12–15), it is important to understand how caspase-8 functions during IAV-induced cell death. However, RIPK3 is also critically involved in IAV-induced pyroptosis, apoptosis, and necroptosis (9, 16), thereby preventing the use of *Casp8*$^{-/-}$*Ripk3*$^{-/-}$ mice as a model to investigate caspase-8 functions during IAV infection. Therefore, the role of caspase-8 in the modulation of cell death during IAV infection remains unclear. Gaining a mechanistic understanding of the regulation of PCD pathways in IAV infection is important for identifying new strategies to prevent the morbidity and mortality associated with this infection.

To study caspase-8 functions during IAV infection, we generated a caspase-8 mutant mouse with a deficiency in caspase-8 autoprocessing, yielding an uncleavable version of the protein (CASP8^{DA}) that, consistent with previous findings, reduces the activation of apoptotic proteins (17). We found that IAV-induced activation of GSDMD and release of the inflammasome-dependent cytokines IL-1β and IL-18 were enhanced in CASP8^{DA} bone marrow-derived macrophages (BMDMs). Mechanistically, caspase-3 was activated downstream of caspase-8 to cleave GSDMD to yield its inactive N-terminal p20 fragment, thus limiting the cytokine release from dying cells. Collectively, our results show that during IAV infection, caspase-8 coordinates the negative regulation of GSDMD-mediated pyroptosis and inhibits proinflammatory cytokine release through the caspase-8–caspase-3 axis.

Materials and Methods

Mice and in vivo infection

Casp8$^{DA/DA}$ (caspase-8$^{D387A/D387A}$) mice were generated by the St. Jude Transgenic/Gene Knockout Shared Resource using CRISPR/Cas9 technology by injecting pronuclear stage C57BL/6J zygotes with a single-guide RNA (Caspase8_D387A_Guide 01, 5′-ATGAATCCACTTCTAAAGTGNGG-3′; 125 ng/μl) designed to introduce a dsDNA break into exon 7 of the *Casp8* gene, human codon-optimized Cas9 mRNA transcripts (50 ng/μl), and a 200-nucleotide ssDNA molecule containing the desired mutations (*Casp8*–D387A homology-directed repair, 5′-GAAAGTCTGCCTCATCCGGAATATAGTTCTTGTGAGATGAGCTCGCCACTTCTAAAGTGTGGTTCTGTTGCTCGAAGCCTGCCTCATCAGGCACTC-3′). To facilitate the identification of founder mice and genotyping, silent substitutions generating an SacI restriction site (5′-GAGCTC-3′) were also introduced. Zygotes were surgically transplanted into the oviducts of pseudopregnant CD1 females, and newborn mice carrying the *Casp8* D387A allele were identified by PCR followed by Sanger sequencing using forward primer 5′-GAAGGAGGCCTCCATCTATGACC-3′ and reverse primer 5′-GCTCTAACCACAGAAATGAGTAAGGAAGC-3′.

Casp3$^{-/-}$ (18), *Casp7*$^{-/-}$ (19), *Ripk3*$^{-/-}$ (20), *Casp8*$^{-/-}$*Ripk3*$^{-/-}$ (7), *Gsdmd*$^{-/-}$ (21), *Zbp1*$^{-/-}$ (22), and ASC-Citrine (JAX 030743) (23) mice have been described previously. IAV infection was performed using a sublethal dose (around 50 PFU of IAV PR8 strain) as previously described (24). Animal studies were conducted under protocols approved by the St. Jude Children's Research Hospital Committee on the Use and Care of Animals.

BMDM culture and in vitro infection

Primary BMDMs were cultured and infected with IAV (multiplicity of infection [MOI] = 20, unless otherwise indicated) as previously described (24). The caspase-3 inhibitor (Z-DEVD-FMK, Selleckchem S7312) was added at 25 μM 6 h postinfection (hpi) where indicated, and samples were collected at 12 hpi.

Immunoblot and cytokine measurement

Immunoblotting for in vitro samples was performed as previously described (24, 25). For immunoblotting of in vivo samples, day 3 postinfection lung tissue was used. The Abs used were anti–caspase-1 (AdipoGen, AG-20B-0042, 1:2000), anti–caspase-3 (Cell Signaling Technology [CST], #9662, 1:1000), anti-cleaved caspase-3 (CST, #9661, 1:1000), anti–caspase-7 (CST, #9492, 1:1000), anti-cleaved caspase-7 (CST, #9491, 1:1000), anti–caspase-8 (CST, #4927, 1:1000),

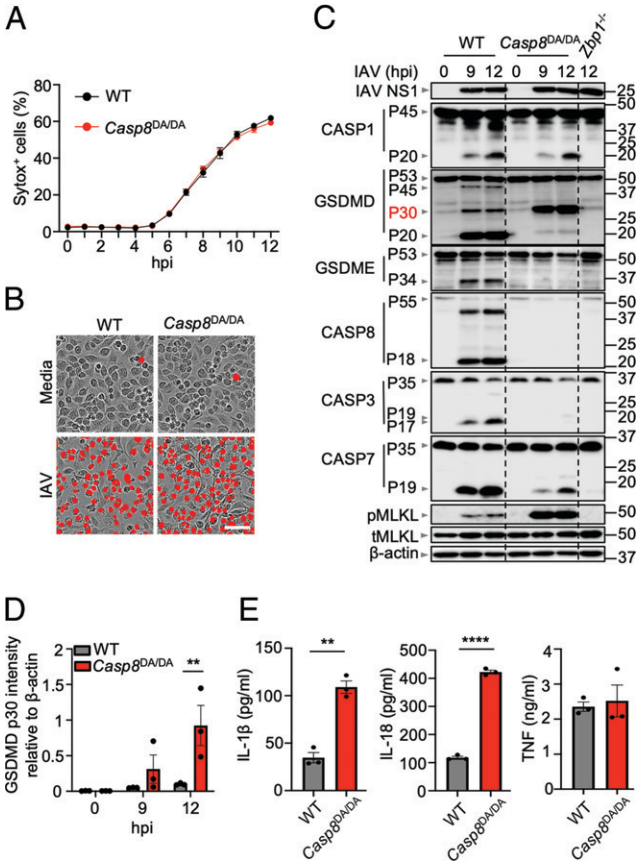

FIGURE 1. Enhanced GSDMD activation and release of IL-1β and IL-18 in *Casp8*$^{DA/DA}$ BMDMs during IAV infection. WT and *Casp8*$^{DA/DA}$ BMDMs were infected with IAV PR8 (MOI = 20). (**A**) Real-time monitoring of cell death; (**B**) representative images of cell death at 12 hpi (red mask denotes dead cells); (**C**) immunoblot analysis of indicated cell death markers (red text denotes the active fragment of GSDMD); (**D**) densitometry measurement of the intensity of the active p30 GSDMD band from three independent replicates normalized to the intensity of β-actin; and (**E**) IL-1β, IL-18, and TNF levels in the cell culture supernatant at 12 hpi. Scale bar, 50 μm (B). Data are presented as mean ± SEM (A, D, E) from at least three independent experiments with individual mice in each experiment. $^{**}p < 0.01$, $^{****}p < 0.0001$ (Student *t* test).

anti-cleaved caspase-8 (CST, #8592, 1:1000), anti-pMLKL (CST, #37333, 1:1000), anti-MLKL (Abgent, AP14272b, 1:1000), anti-GSDMD (Abcam, ab209845, 1:1000), anti-gasdermin E (GSDME) (Abcam, ab215191, 1:1000), anti–β-actin (Proteintech, 66009-1-IG, 1:5000), and HRP-conjugated secondary Abs (Jackson ImmunoResearch Laboratories, anti-rabbit [111-035-047], 1:5000; anti-mouse [315-035-047], 1:5000). Densitometry of the bands was quantified in ImageJ and normalized to the band density of β-actin. IL-18 release was measured using ELISA kits (Invitrogen, BMS618-3). IL-1β and TNF release were measured by multiplex ELISAs (Millipore MCYTOMAG-70K). Cytokines from bronchoalveolar lavage fluid were measured as previously described (26).

Real-time cell death and caspase-3/7 activity analysis

Real-time cell death analysis was performed as previously described (24). Caspase-3/7 activity analysis was monitored following the same protocol using the Incucyte Caspase-3/7 Red reagent (Essen BioScience, 4704).

Confocal microscopy

After the indicated treatment, BMDMs were fixed with 4% paraformaldehyde, permeabilized in PBS with 0.05% Triton, blocked with 1% skim milk in PBS, and stained with the primary Abs conjugated to Alexa Fluor 488, anti-cleaved CASP3 (CST #9669), and anti-ASC (Millipore 2EI-7), followed by staining with the secondary Alexa Fluor 647 anti-mouse IgG Ab and DAPI. Images were acquired using a Marianis spinning disk confocal microscope (Intelligent Imaging Innovations).

Statistical analysis

GraphPad Prism v9.0 software was used for data analysis. Statistical significance was determined by Student *t* test between two groups or one-way ANOVA for three or more groups and log-rank test for survival analysis. Mean ± SEM of the data is presented.

Results and Discussion

IAV infection triggers pyroptosis, apoptosis, and necroptosis (PANoptosis) in BMDMs (9). Given the important role of caspase-8 in balancing PCD pathways during embryogenesis (27, 28), we sought to understand the function of caspase-8 during IAV infection. To first determine whether caspase-8 is involved in regulating PCD pathways during IAV infection, we infected wild-type (WT), *Casp8*$^{-/-}$*Ripk3*$^{-/-}$ and *Ripk3*$^{-/-}$ BMDMs with IAV and monitored the activation of key molecules involved in PANoptosis. Infected WT cells showed activation of caspase-1, GSDMD and GSDME (pyroptotic markers), caspase-8, caspase-3, and caspase-7 (apoptotic markers), and MLKL (necroptotic marker), whereas infected *Casp8*$^{-/-}$*Ripk3*$^{-/-}$ BMDMs displayed minimal or no activation of these markers at the same time points (Supplemental Fig. 1). However, we also observed a notable reduction in the activation of each of these markers in *Ripk3*$^{-/-}$ BMDMs infected with IAV (Supplemental Fig. 1), as previously reported (9, 16). Thus, the role of RIPK3 in IAV-induced cell death prevents interpretation of the caspase-8 function in *Casp8*$^{-/-}$*Ripk3*$^{-/-}$ cells.

To overcome this obstacle and enable evaluation of the role of caspase-8 in IAV-induced cell death, we next generated *Casp8*$^{DA/DA}$ mice, where the caspase-8 autoprocessing function was inhibited by replacing aspartic acid 387 (D387) with alanine (CASP8^{DA}) (Supplemental Fig. 2), yielding an uncleavable form of the protein. Upon infection with IAV, WT and *Casp8*$^{DA/DA}$ BMDMs showed comparable numbers of dead cells and similar rates of viral protein production (Fig. 1A–C). However, further biochemical examination of PCD pathways showed key differences in the activation of pyroptotic, apoptotic, and necroptotic proteins in IAV-infected *Casp8*$^{DA/DA}$ BMDMs (Fig. 1C). Autoprocessing of caspase-8 is essential for the downstream activation of caspase-3 and -7 in the extrinsic apoptosis pathway (17) and for the subsequent activation of GSDME (29). *Casp8*$^{DA/DA}$ BMDMs showed impaired caspase-3, caspase-7, and GSDME cleavage (Fig. 1C). However, although inflammasome activation (caspase-1 cleavage) remained consistent between WT and *Casp8*$^{DA/DA}$ BMDMs, an increase in the GSDMD activation (p30 fragment) was observed in *Casp8*$^{DA/DA}$ BMDMs (Fig. 1C, 1D). In addition, phosphorylation of MLKL, a hallmark of necroptosis, was also increased (Fig. 1C). Activated GSDMD mediates the release of processed IL-1β and IL-18 downstream of caspase-1 activation (30). Indeed, the amounts of IL-1β and IL-18, but not TNF, were significantly higher in the supernatant at 12 hpi in *Casp8*$^{DA/DA}$ BMDMs compared with WT BMDMs, consistent with the enhanced activation of the GSDMD pore-forming molecule (Fig. 1E). The equivalent cell death, increased GSDMD activation, and higher IL-1β and IL-18 release were consistently observed in *Casp8*$^{DA/DA}$ BMDMs compared with WT across different IAV MOIs and at different time points of infection (Supplemental Fig. 3).

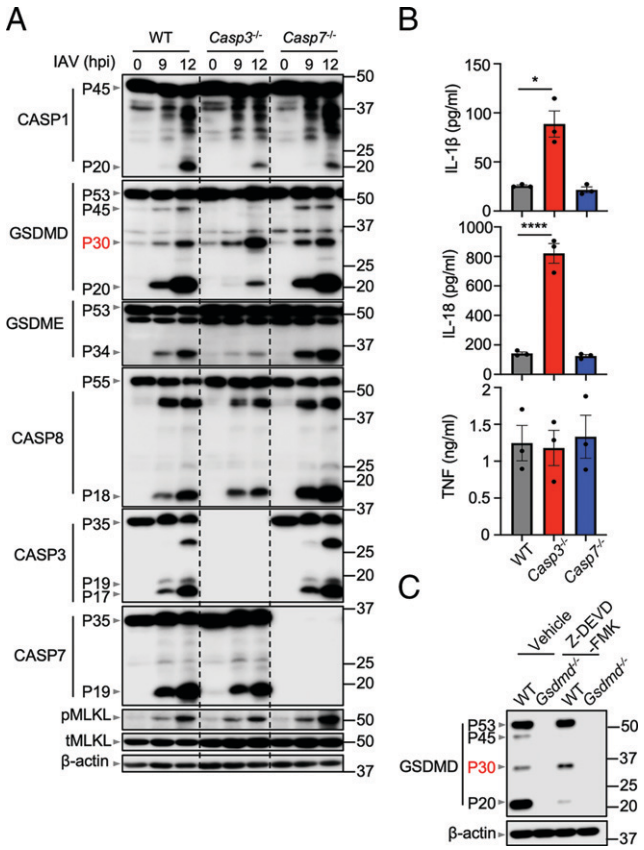

FIGURE 2. Caspase-3, but not caspase-7, suppresses GSDMD activation and release of IL-1β and IL-18 during IAV infection. BMDMs from the indicated genotypes were infected with IAV PR8 (MOI = 20). (**A**) Immunoblot analysis of indicated cell death markers; (**B**) IL-1β, IL-18, and TNF levels in the cell culture supernatant at 12 hpi; and (**C**) immunoblot analysis of GSDMD with 25 μM caspase-3 inhibitor (Z-DEVD-FMK) treatment during IAV infection. Red text denotes the active form of GSDMD. Data are presented as mean ± SEM (B) from at least three independent experiments with individual mice in each experiment. $^{*}p < 0.05$, $^{****}p < 0.0001$ (one-way ANOVA).

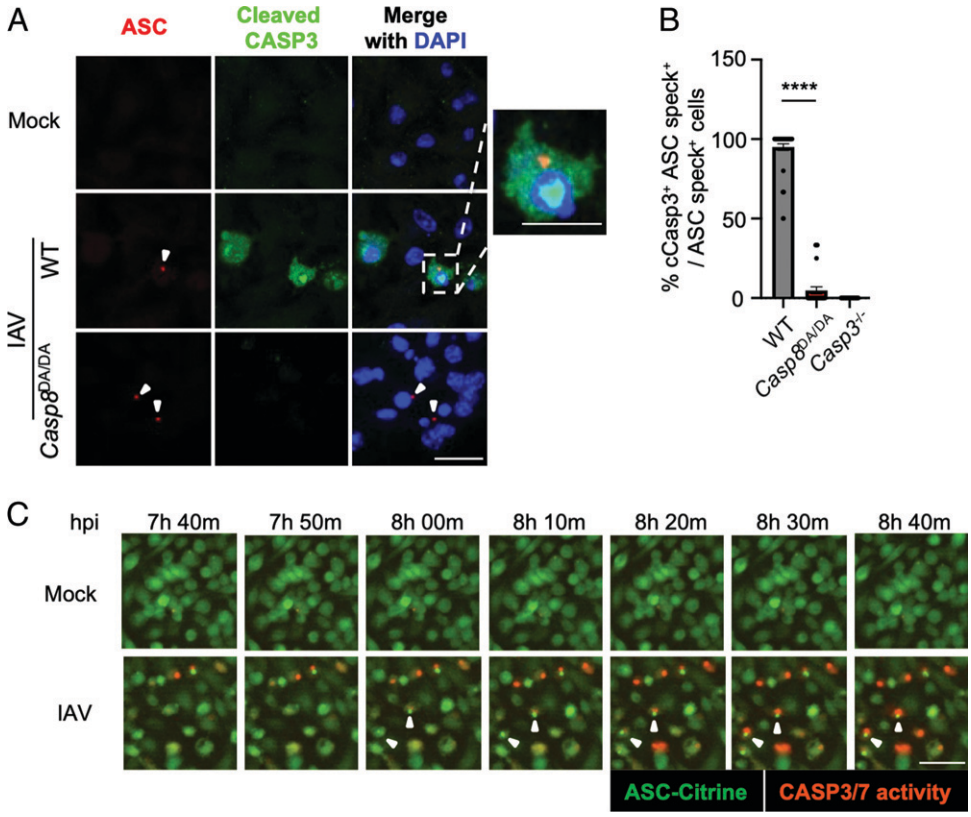

FIGURE 3. Parallel pyroptotic and apoptotic pathways in individual cells during IAV infection. (**A**) WT, *Casp8*$^{DA/DA}$, and *Casp3*$^{-/-}$ BMDMs were infected with IAV PR8 (MOI = 20) for 12 h and stained for ASC and cleaved caspase-3. Scale bar, 20 μm or 10 μm (inset). Arrows denote ASC specks. (**B**) Quantification of the cell staining pattern in WT, *Casp8*$^{DA/DA}$, and *Casp3*$^{-/-}$ cells. Each dot represents one frame containing at least one ASC speck (over 500 cells from each genotype were examined). (**C**) Live-cell imaging of ASC-citrine BMDMs during IAV infection in the presence of caspase-3/7 activity probe. Scale bar, 50 μm. Arrows denote ASC specks. Data are presented as mean ± SEM (B) and are representative of at least three independent experiments with individual mice in each experiment. ****$p < 0.0001$ (one-way ANOVA).

To understand the mechanism underlying the increased activation of GSDMD and release of IL-1β and IL-18 in *Casp8*$^{DA/DA}$ BMDMs during IAV infection, we investigated the role of other cell death molecules in the cleavage of GSDMD under these conditions. Caspase-3 and -7 can cleave full-length GSDMD at its N-terminal D87 residue to form an inactive p45 fragment in a recombinant system (31). We also observed a p45 fragment in WT BMDMs upon IAV infection, and the formation of this fragment was decreased in *Casp8*$^{DA/DA}$ BMDMs (Fig. 1C). Moreover, we observed a p20 GSDMD fragment that was inversely correlated with the formation of the active p30 fragment at 9 and 12 hpi. Dual cleavage of GSDMD by both caspase-1 and caspase-3/7 can generate a p20 fragment, as suggested by a previous report in cells overexpressing both caspase-1 and caspase-3 (32). We therefore hypothesized that the increased GSDMD p30 formation observed in *Casp8*$^{DA/DA}$ BMDMs after IAV infection was due to a lack of caspase-3/7–mediated cleavage, as activation of caspase-3/7 was substantially reduced in *Casp8*$^{DA/DA}$ BMDMs. To test this possibility, we infected BMDMs from either *Casp3*$^{-/-}$ or *Casp7*$^{-/-}$ mice with IAV and analyzed the activation of cell death markers and cytokine release. The robust increase in the formation of the active GSDMD p30 fragment and decrease in the formation of the p20 fragment seen in *Casp8*$^{DA/DA}$ BMDMs (Fig. 1C) were seen in *Casp3*$^{-/-}$ but not in *Casp7*$^{-/-}$ BMDMs postinfection (Fig. 2A). Additionally, the release of IL-1β and IL-18 was also significantly increased in *Casp3*$^{-/-}$ but not in *Casp7*$^{-/-}$ BMDMs, whereas the secretion of the GSDMD-independent cytokine TNF remained comparable between WT, *Casp3*$^{-/-}$, and *Casp7*$^{-/-}$ BMDMs (Fig. 2B). Despite the increase in the release of IL-1β and IL-18, phosphorylation of the necroptosis marker MLKL was not changed in *Casp3*$^{-/-}$ (Fig. 2A), suggesting that the release of these cytokines is independent of MLKL in *Casp3*$^{-/-}$ cells. To further confirm that enzymatic activity of caspase-3 is critical to modulate GSDMD activation, we treated WT and *Gsdmd*$^{-/-}$ cells with the caspase-3 inhibitor Z-DEVD-FMK. We observed that inhibition of caspase-3 activity increased the formation of the active GSDMD p30 fragment and reduced the formation of the inactive form p20 (Fig. 2C). These observations suggest an inhibitory role for the caspase-8–caspase-3 axis to keep GSDMD activity in check and limit the release of proinflammatory cytokines processed by caspase-1.

Based on the known cleavage sites of the caspases, the presence of both activated caspase-1 and caspase-3 in the same cell could potentially lead to the formation of the GSDMD p20 fragment. Although concerted activation of caspase-8 and caspase-3 can be observed during AIM2, NLRP3, NLRP1b, and NLRC4 inflammasome activation, in particular under conditions where caspase-1 or GSDMD are deleted (33–37), caspase-1 and -3 are biochemically activated at the same time in a population of cells during various conditions (10). However, the simultaneous engagement of apoptotic and pyroptotic proteins in a single cell has not been visualized and characterized under physiological conditions. To determine whether apoptotic and pyroptotic processes occur in the same cell at the same time during IAV infection, we first stained the ASC speck, the hallmark of inflammasome/pyroptotic process activation, and cleaved caspase-3, to mark cells with activated apoptotic processes (Fig. 3A). At 12 hpi with IAV, nearly all WT BMDMs observed to contain ASC specks were also positive for cleaved

caspase-3, whereas *Casp8*$^{DA/DA}$ cells containing ASC specks were generally negative for cleaved caspase-3 (Fig. 3A, 3B), consistent with our biochemical observation (Fig. 1C, Supplemental Fig. 3B). To gain further insight into the kinetics of ASC speck formation and the activation of apoptotic caspases, we used BMDMs derived from ASC-citrine mice (23) and performed live-cell imaging in the presence of a fluorogenic caspase-3/7 probe. In line with the confocal observations, IAV-infected cells with ASC specks also frequently showed caspase-3/7 activity (Fig. 3C). The formation of ASC specks generally preceded the emergence of caspase-3/7 activity by less than 10 min (Fig. 3C), suggesting that the onset of pyroptotic and apoptotic pathways occurs together in ASC speck-positive cells during IAV infection. The presence of cleaved caspase-3 in nearly all ASC speck-positive WT cells after IAV infection further supports that caspase-1 and caspase-3 could cleave GSDMD to form the inactive p20 fragment. Together, these findings suggest that the activation of GSDMD is held in check by the caspase-8–caspase-3 axis.

Activation of the NLRP3 inflammasome and IL-1β and IL-18 cytokine release are known to be protective during IAV infection in mice (11–15). Based on the essential role of the caspase-8–caspase-3 axis we observed in regulating GSDMD activation and IL-1β and IL-18 release, we tested the effect of having the uncleavable caspase-8 (*Casp8*$^{DA/DA}$) during IAV infection in vivo. *Casp8*$^{DA/DA}$ mice had improved survival and lost less body weight compared with WT mice during IAV infection (Supplemental Fig. 4A, 4B). Lungs from infected *Casp8*$^{DA/DA}$ mice at day 3 postinfection also had increased GSDMD activation (Supplemental Fig. 4C, 4D) together with increased IL-1β and IL-18 in bronchoalveolar lavage fluid compared with WT mice (Supplemental Fig. 4E, 4F), consistent with our in vitro finding in BMDMs. These findings further suggest that caspase-8 activation negatively regulates pyroptotic effectors in vivo during infection, providing a potential explanation for viral resistance of *Casp3*$^{-/-}$ mice (38).

Overall, our findings showed an anti-inflammatory function of caspase-8 through its autoprocessing during IAV infection. At the cellular level, autoprocessing of caspase-8 leads to activation of caspase-3, which subsequently results in cleavage of GSDMD to produce its inactive form, limiting IL-1β and IL-18 release. The activity of the caspase-8–caspase-3 axis observed in this study may represent a coevolved feature of the virus developed to suppress the host inflammatory response and improve viral propagation, although the specific viral proteins involved in this process require further study. Although mounting evidence shows that the concerted activation of apoptotic and pyroptotic proteins can occur under various conditions (10), our model provides an explanation for the functional consequences from such PCD cross-talk under physiological conditions during viral infection. Improved understanding of this cross-talk and the essential roles of caspase-8 to act as a linchpin in these processes will improve our ability to modulate the immune system to limit viral replication and prevent pathogenesis.

Acknowledgments

We thank all members of the Kanneganti laboratory for discussions. We also thank R. Tweedell for scientific editing and writing support.

Disclosures

The authors have no financial conflicts of interest.

References

1. Gurung, P., P. K. Anand, R. K. Malireddi, L. Vande Walle, N. Van Opdenbosch, C. P. Dillon, R. Weinlich, D. R. Green, M. Lamkanfi, and T. D. Kanneganti. 2014. FADD and caspase-8 mediate priming and activation of the canonical and noncanonical Nlrp3 inflammasomes. *J. Immunol.* 192: 1835–1846.
2. Orning, P., D. Weng, K. Starheim, D. Ratner, Z. Best, B. Lee, A. Brooks, S. Xia, H. Wu, M. A. Kelliher, et al. 2018. Pathogen blockade of TAK1 triggers caspase-8-dependent cleavage of gasdermin D and cell death. *Science* 362: 1064–1069.
3. Sarhan, J., B. C. Liu, H. I. Muendlein, P. Li, R. Nilson, A. Y. Tang, A. Rongvaux, S. C. Bunnell, F. Shao, D. R. Green, and A. Poltorak. 2018. Caspase-8 induces cleavage of gasdermin D to elicit pyroptosis during *Yersinia* infection. *Proc. Natl. Acad. Sci. USA.* DOI: 10.1073/pnas.1809548115.
4. Stennicke, H. R., J. M. Jürgensmeier, H. Shin, Q. Deveraux, B. B. Wolf, X. Yang, Q. Zhou, H. M. Ellerby, L. M. Ellerby, D. Bredesen, et al. 1998. Pro-caspase-3 is a major physiologic target of caspase-8. *J. Biol. Chem.* 273: 27084–27090.
5. Newton, K., K. E. Wickliffe, D. L. Dugger, A. Maltzman, M. Roose-Girma, M. Dohse, L. Kőműves, J. D. Webster, and V. M. Dixit. 2019. Cleavage of RIPK1 by caspase-8 is crucial for limiting apoptosis and necroptosis. *Nature* 574: 428–431.
6. Kaiser, W. J., J. W. Upton, A. B. Long, D. Livingston-Rosanoff, L. P. Daley-Bauer, R. Hakem, T. Caspary, and E. S. Mocarski. 2011. RIP3 mediates the embryonic lethality of caspase-8-deficient mice. *Nature* 471: 368–372.
7. Oberst, A., C. P. Dillon, R. Weinlich, L. L. McCormick, P. Fitzgerald, C. Pop, R. Hakem, G. S. Salvesen, and D. R. Green. 2011. Catalytic activity of the caspase-8-FLIP(L) complex inhibits RIPK3-dependent necrosis. *Nature* 471: 363–367.
8. Orozco, S., and A. Oberst. 2017. RIPK3 in cell death and inflammation: the good, the bad, and the ugly. *Immunol. Rev.* 277: 102–112.
9. Kuriakose, T., S. M. Man, R. K. Malireddi, R. Karki, S. Kesavardhana, D. E. Place, G. Neale, P. Vogel, and T. D. Kanneganti. 2016. ZBP1/DAI is an innate sensor of influenza virus triggering the NLRP3 inflammasome and programmed cell death pathways. *Sci. Immunol.* DOI: 10.1126/sciimmunol.aag2045.
10. Christgen, S., M. Zheng, S. Kesavardhana, R. Karki, R. K. S. Malireddi, B. Banoth, D. E. Place, B. Briard, B. R. Sharma, S. Tuladhar, et al. 2020. Identification of the PANoptosome: a molecular platform triggering pyroptosis, apoptosis, and necroptosis (PANoptosis). *Front. Cell. Infect. Microbiol.* DOI: 10.3389/fcimb.2020.00237.
11. Kanneganti, T. D., M. Body-Malapel, A. Amer, J. H. Park, J. Whitfield, L. Franchi, Z. F. Taraporewala, D. Miller, J. T. Patton, N. Inohara, and G. Núñez. 2006. Critical role for Cryopyrin/Nalp3 in activation of caspase-1 in response to viral infection and double-stranded RNA. *J. Biol. Chem.* 281: 36560–36568.
12. Thomas, P. G., P. Dash, J. R. Aldridge, Jr., A. H. Ellebedy, C. Reynolds, A. J. Funk, W. J. Martin, M. Lamkanfi, R. J. Webby, K. L. Boyd, et al. 2009. The intracellular sensor NLRP3 mediates key innate and healing responses to influenza A virus via the regulation of caspase-1. *Immunity* 30: 566–575.
13. Ichinohe, T., H. K. Lee, Y. Ogura, R. Flavell, and A. Iwasaki. 2009. Inflammasome recognition of influenza virus is essential for adaptive immune responses. *J. Exp. Med.* 206: 79–87.
14. Schmitz, N., M. Kurrer, M. F. Bachmann, and M. Kopf. 2005. Interleukin-1 is responsible for acute lung immunopathology but increases survival of respiratory influenza virus infection. *J. Virol.* 79: 6441–6448.
15. Liu, B., I. Mori, M. J. Hossain, L. Dong, K. Takeda, and Y. Kimura. 2004. Interleukin-18 improves the early defence system against influenza virus infection by augmenting natural killer cell-mediated cytotoxicity. *J. Gen. Virol.* 85: 423–428.
16. Nogusa, S., R. J. Thapa, C. P. Dillon, S. Liedmann, T. H. Oguin III, J. P. Ingram, D. A. Rodriguez, R. Kosoff, S. Sharma, O. Sturm, et al. 2016. RIPK3 activates parallel pathways of MLKL-driven necroptosis and FADD-mediated apoptosis to protect against influenza A virus. *Cell Host Microbe* 20: 13–24.
17. Kang, T. B., G. S. Oh, E. Scandella, B. Bolinger, B. Ludewig, A. Kovalenko, and D. Wallach. 2008. Mutation of a self-processing site in caspase-8 compromises its apoptotic but not its nonapoptotic functions in bacterial artificial chromosome-transgenic mice. *J. Immunol.* 181: 2522–2532.
18. Zheng, T. S., S. Hunot, K. Kuida, T. Momoi, A. Srinivasan, D. W. Nicholson, Y. Lazebnik, and R. A. Flavell. 2000. Deficiency in caspase-9 or caspase-3 induces compensatory caspase activation. *Nat. Med.* 6: 1241–1247.
19. Lakhani, S. A., A. Masud, K. Kuida, G. A. Porter, Jr., C. J. Booth, W. Z. Mehal, I. Inayat, and R. A. Flavell. 2006. Caspases 3 and 7: key mediators of mitochondrial events of apoptosis. *Science* 311: 847–851.
20. Newton, K., X. Sun, and V. M. Dixit. 2004. Kinase RIP3 is dispensable for normal NF-kappa Bs, signaling by the B-cell and T-cell receptors, tumor necrosis factor receptor 1, and Toll-like receptors 2 and 4. *Mol. Cell. Biol.* 24: 1464–1469.
21. Karki, R., E. Lee, D. Place, P. Samir, J. Mavuluri, B. R. Sharma, A. Balakrishnan, R. K. S. Malireddi, R. Geiger, Q. Zhu, et al. 2018. IRF8 regulates transcription of Naips for NLRC4 inflammasome activation. *Cell* 173: 920–933.e13.
22. Ishii, K. J., T. Kawagoe, S. Koyama, K. Matsui, H. Kumar, T. Kawai, S. Uematsu, O. Takeuchi, F. Takeshita, C. Coban, and S. Akira. 2008. TANK-binding kinase-1 delineates innate and adaptive immune responses to DNA vaccines. *Nature* 451: 725–729.
23. Tzeng, T. C., S. Schattgen, B. Monks, D. Wang, A. Cerny, E. Latz, K. Fitzgerald, and D. T. Golenbock. 2016. A fluorescent reporter mouse for inflammasome assembly demonstrates an important role for cell-bound and free ASC specks during in vivo infection. *Cell Rep.* 16: 571–582.
24. Zheng, M., R. Karki, P. Vogel, and T. D. Kanneganti. 2020. Caspase-6 is a key regulator of innate immunity, inflammasome activation, and host defense. *Cell* 181: 674–687.e13.
25. Karki, R., B. R. Sharma, E. Lee, B. Banoth, R. K. S. Malireddi, P. Samir, S. Tuladhar, H. Mummareddy, A. R. Burton, P. Vogel, and T. D. Kanneganti. 2020. Interferon

regulatory factor 1 regulates PANoptosis to prevent colorectal cancer. *JCI Insight*. DOI: 10.1172/jci.insight.136720.
26. Lee, S., A. Ishitsuka, M. Noguchi, M. Hirohama, Y. Fujiyasu, P. P. Petric, M. Schwemmle, P. Staeheli, K. Nagata, and A. Kawaguchi. 2019. Influenza restriction factor MxA functions as inflammasome sensor in the respiratory epithelium. *Sci. Immunol*. DOI: 10.1126/sciimmunol.aau4643.
27. Newton, K., K. E. Wickliffe, A. Maltzman, D. L. Dugger, R. Reja, Y. Zhang, M. Roose-Girma, Z. Modrusan, M. S. Sagolla, J. D. Webster, and V. M. Dixit. 2019. Activity of caspase-8 determines plasticity between cell death pathways. *Nature* 575: 679–682.
28. Fritsch, M., S. D. Günther, R. Schwarzer, M. C. Albert, F. Schorn, J. P. Werthenbach, L. M. Schiffmann, N. Stair, H. Stocks, J. M. Seeger, et al. 2019. Caspase-8 is the molecular switch for apoptosis, necroptosis and pyroptosis. *Nature* 575: 683–687.
29. Wang, Y., W. Gao, X. Shi, J. Ding, W. Liu, H. He, K. Wang, and F. Shao. 2017. Chemotherapy drugs induce pyroptosis through caspase-3 cleavage of a gasdermin. *Nature* 547: 99–103.
30. Shi, J., Y. Zhao, K. Wang, X. Shi, Y. Wang, H. Huang, Y. Zhuang, T. Cai, F. Wang, and F. Shao. 2015. Cleavage of GSDMD by inflammatory caspases determines pyroptotic cell death. *Nature* 526: 660–665.
31. Taabazuing, C. Y., M. C. Okondo, and D. A. Bachovchin. 2017. Pyroptosis and apoptosis pathways engage in bidirectional crosstalk in monocytes and macrophages. *Cell Chem. Biol.* 24: 507–514.e4.
32. Chen, K. W., B. Demarco, R. Heilig, K. Shkarina, A. Boettcher, C. J. Farady, P. Pelczar, and P. Broz. 2019. Extrinsic and intrinsic apoptosis activate pannexin-1 to drive NLRP3 inflammasome assembly. *EMBO J.* DOI: 10.15252/embj.2019101638.
33. Sagulenko, V., S. J. Thygesen, D. P. Sester, A. Idris, J. A. Cridland, P. R. Vajjhala, T. L. Roberts, K. Schroder, J. E. Vince, J. M. Hill, et al. 2013. AIM2 and NLRP3 inflammasomes activate both apoptotic and pyroptotic death pathways via ASC. *Cell Death Differ*. 20: 1149–1160.
34. Lee, B. L., K. M. Mirrashidi, I. B. Stowe, S. K. Kummerfeld, C. Watanabe, B. Haley, T. L. Cuellar, M. Reichelt, and N. Kayagaki. 2018. ASC- and caspase-8-dependent apoptotic pathway diverges from the NLRC4 inflammasome in macrophages. *Sci. Rep.* DOI: 10.1038/s41598-018-21998-3.
35. Van Opdenbosch, N., H. Van Gorp, M. Verdonckt, P. H. V. Saavedra, N. M. de Vasconcelos, A. Gonçalves, L. Vande Walle, D. Demon, M. Matusiak, F. Van Hauwermeiren, et al. 2017. Caspase-1 engagement and TLR-induced c-FLIP expression suppress ASC/caspase-8-dependent apoptosis by inflammasome sensors NLRP1b and NLRC4. *Cell Rep.* 21: 3427–3444.
36. Puri, A. W., P. Broz, A. Shen, D. M. Monack, and M. Bogyo. 2012. Caspase-1 activity is required to bypass macrophage apoptosis upon *Salmonella* infection. *Nat. Chem. Biol.* 8: 745–747.
37. Pierini, R., C. Juruj, M. Perret, C. L. Jones, P. Mangeot, D. S. Weiss, and T. Henry. 2012. AIM2/ASC triggers caspase-8-dependent apoptosis in *Francisella*-infected caspase-1-deficient macrophages. *Cell Death Differ*. 19: 1709–1721.
38. Ning, X., Y. Wang, M. Jing, M. Sha, M. Lv, P. Gao, R. Zhang, X. Huang, J. M. Feng, and Z. Jiang. 2019. Apoptotic caspases suppress type I interferon production via the cleavage of cGAS, MAVS, and IRF3. *Mol. Cell* 74: 19–31.e7.